Thermal entanglement properties of small spin clusters

Indrani Bose and Amit Tribedi

2nd February 2008

Department of Physics
Bose Institute
93/1, Acharya Prafulla Chandra Road
Kolkata - 700 009, India

Abstract

Exchange interactions in spin systems can give rise to quantum entanglement in the ground and thermal states of the systems. In this paper, we consider a spin tetramer, with spins of magnitude $\frac{1}{2}$, in which the spins interact via nearest-neighbour, diagonal and four-spin interactions of strength J_1, J_2 and K respectively. The ground and thermal state entanglement properties of the tetramer are calculated analytically in the various limiting cases. Both bipartite and multipartite entanglements are considered and a signature of quantum phase transition (QPT), in terms of the entanglement ratio, is identified. The first order QPT is accompanied by discontinuities in the nearest-neighbour and diagonal concurrences. The magnetic properties of a $S = \frac{1}{2}$ AFM polyoxovanadate compound, $V12$, are well explained by tetramers, with $J_2 = 0$, $K = 0$, in which the spins interact via the isotropic Heisenberg exchange interaction Hamiltonian. Treating the magnetic susceptibility χ as an entanglement witness (EW), an estimate of the lower bound of the critical entanglement temperature, T_c, above which the entanglement between two individual spins disappears in the experimental compound, is determined. Two other cases considered include the symmetric tetramer, i.e. tetrahedron ($J_1 = J_2$, K=0) and the symmetric trimer. In both the cases, there is no entanglement between a pair of spins in the thermal state but multipartite entanglement is present. A second EW based on energy provides an estimate of the entanglement temperature, T_E, below which the thermal state is definitely entangled. This EW detects bipartite entanglement in the case of the tetramer describing a square of spins (the case of $V12$) and multipartite entanglement in the cases of the tetrahedron and the symmetric trimer.

I. Introduction

Entanglement is a fundamental property of quantum mechanical systems and gives rise to an excess of correlations in a system over and above those expected from classical considerations [1]. A pure state is said to be entangled if it does not factorize , i.e., cannot be written as a product of individual wave functions. A well -known example of an entangled state is the singlet state of two spin-$\frac{1}{2}$ particles, $\frac{1}{\sqrt{2}}\left(|\uparrow\downarrow\rangle - |\downarrow\uparrow\rangle\right)$, which cannot be written as a product of the spin states of individual spins. Measurement on one component of an entangled pair fixes the state of the other implying non-local correlations. In the case of a mixed state, entanglement occurs if the density matrix is not a convex sum of product states. The importance of entanglement derives from its essential role in applications related to quantum information and communication. Candidate systems for implementing the application protocols include spin systems in which exchange interactions give rise to entanglement [2, 3, 4, 5].

Entanglement is a resource which can be created, manipulated and destroyed. It can be of different types, e.g., bipartite, multipartite, localizable [6], zero-temperature, finite-temperature etc. for which appropriate quantification measures are available. Bipartite (multipartite) entanglement involves two (more than two) subsystems. The entanglement between a pair of spins belonging to a chain of interacting spins provides an example of bipartite entanglement. Bipartite and to a lesser extent multipartite entanglement properties of a variety of spin models have been studied so far at both zero and finite temperatures and including an external magnetic field [7, 8, 9, 10, 11, 12, 13, 14, 15, 16]. These studies show that the amount of entanglement can be changed by changing the temperature T and/or the external magnetic field. Since entanglement involves non-local correlations of purely quantum origin, an issue of considerable interest is whether entanglement develops special features in the vicinity of a quantum phase transition (QPT). A QPT occurs at $T = 0$ and is brought about by tuning some system parameter, say, the exchange interaction strength or an external variable like the magnetic field to a critical value [17]. In a QPT, the ground state of the system undergoes qualitative changes which in turn affects the entanglement properties in the ground state. Some recent studies have explored the relation between entanglement and QPT in a variety of spin models and the main conclusion is that certain entanglement-related quantities exhibit features like scaling and singularity in the vicinity of a quantum critical point (QCP) [15, 16, 18, 19, 20, 21, 22]. In the case of first-order QPTs, the ground state concurrences may change discontinuously at the transition point [23, 24, 25, 26]. The influence of quantum criticality extends also to finite temperatures so that measurements of appropriate observables provide signatures of QPT. At finite T, the system in thermal equilibrium is described by the density operator, $\rho\left(T\right) = \frac{1}{Z}exp\left(-\frac{H}{k_B T}\right)$, where H is the Hamiltonian, Z the partition function and k_B the Boltzmann constant. A thermal state remains entangled upto a critical temperature T_c beyond which the state becomes separable, i.e., the entanglement falls to zero. Experimental demonstrations of entanglement are mostly confined to the microworld, i.e., to systems consisting of a few photons, atoms or ions. There is now experimental evidence that entanglement can also affect the macroscopic properties of solids. This has been shown in the insulating magnetic compound $LiHo_xY_{1-x}F_4$ the specific heat and the susceptibility data of which can only be explained if quantum entanglement of the relevant states is explicitly taken into account [27, 28]. Measures of thermal entanglement based on the thermal density matrix require a knowledge of both the eigenvalues and the eigenvectors of H. On the other hand, there are suggestions that macroscopic thermodynamic observables can serve as entanglement witnesses so that a measurement of these quantities can provide the evidence for entanglement [11, 28, 29, 30, 31]. An entanglement witness (EW) is an observable the expectation value of which is positive in unentangled, i.e., separable states and negative in entangled states [32, 33, 34]. The thermodynamic observables which have been proposed as EWs include internal energy and magnetization and magnetic susceptibility [28, 31]. The latter has been used as an EW in the spin-$\frac{1}{2}$ alternating bond antiferromagnet $Cu(NO_3)_2 2.5D_2O(CN)$. The compound can be considered as a chain of uncoupled spin dimers since the ratio of the inter-dimer to the intra-dimer exchange interaction strengths is approximately 0.24, i.e., low. For separable (unentangled) states, the magnetic susceptibility obeys the inequality

$$\chi \geq \frac{(g\mu_B)^2 N}{k_B T} \frac{1}{6} \tag{1}$$

where g is the Landé splitting factor, μ_B the Bohr magneton and N the number of spins in the system. Entanglement is present in the system if the inequality in (1) is violated. The intersection point of the curve representing the EW (equality in (1)) and the experimental χ versus T curve defines the critical temperature T_c below which entanglement is present in the system. The experimental estimate of $T_c \simeq 5K$ is in good agreement with the theoretical value of the critical temperature at which the pairwise thermal entanglement (entanglement between two spins), as measured by the concurrence, falls to zero.

Determination of the entanglement properties of an interacting spin system is a theoretical challenge as the eigenstates and eigenvalues are not known exactly when the number of spins is large. Most of the calculations are confined to systems containing a few spins so that exact diagonalization is possible. Studies on finite quantum spin systems acquire significant relevance in the context of molecular or nanomagnets. In such magnetic systems, the dominant exchange interactions are often confined to small spin clusters. The inter-cluster exchange interactions are much weaker in comparison so that the compounds can be assumed to consist of independent spin clusters. A recent study provides a number of examples of molecular magnets the thermodynamic and neutron scattering properties of which can be well described by small spin clusters like dimers, trimers and tetramers [35]. As in Ref. [28], one can study the entanglement properties of the molecular magnets by treating the susceptibility χ as an EW. The earlier work dealt with spin dimers for which only pairwise entanglement is possible. In this paper, we consider clusters of three (trimer) and four (tetramer) spins in which pairwise entanglement between individual spins does not exhaust the total entanglement. The tetramer Hamiltonian contains both bilinear and four-spin interactions. The ground state and thermal entanglement properties of the tetramers are determined analytically. The influence of multispin interactions on entanglement is further determined. The system exhibits QPTs at special values of the exchange interaction strengths. A signature of the QPT via the so-called entanglement ratio is identified. A distinct signature of first order QPT is provided by jumps in the amounts of entanglement associated with n.n. and diagonal spin pairs. The magnetic properties of the polyoxovanadate compound, $(NHEt)_3\left[V_8^{IV}V_4^{V}As_8O_{40}\left(H_2O\right)\right].H_2O$ (designated as $V12$) are well explained by spin$-\frac{1}{2}$ AFM tetramers, with only nearest-neighbour (n.n.) interactions, and described by the isotropic Heisenberg exchange interaction Hamiltonian [35, 36]. The experimental data on the magnetic susceptibility of this compound are available. Treating χ as an EW, the critical entanglement temperature, T_c, below which entanglement is certainly present in the system, is determined. The cases of the $S=\frac{1}{2}$ AFM symmetric trimer and tetrahedron are also considered.

Dowling et al.[33] have introduced the concept of the entanglement gap, defined to be the difference in the energies of the minimum energy, E_{sep}, that a separable state may attain and the ground state energy E_0. If the energy of the system falls within the entanglement gap, the state of the system is entangled. The entanglement gap temperature, T_E, is defined to be the temperature at which the thermal energy $U(T_E)=E_{sep}$, the minimum separable energy. Below T_E, the thermal state of the system is bound to be entangled. We obtain an estimate of T_E in the cases of a single square of spins (the case of $V12$), a tetrahedron and a symmetric trimer. In the last two cases the critical entanglement temperature T_c, determined by using χ as an EW, is identical to the entanglement gap temperature T_E.

II. Entanglement properties of $S=\frac{1}{2}$ AFM tetramer

We consider a tetramer of spins of magnitude $\frac{1}{2}$ (Fig. 1) described by the AFM Heisenberg exchange interaction Hamiltonian

$$\begin{aligned} H \; = \; & J_1\left(S_1.S_2+S_2.S_3+S_3.S_4+S_4.S_1\right)+J_2(S_1.S_3+S_2.S_4) \\ & +K_1(S_1.S_2)(S_3.S_4)+K_1(S_2.S_3)(S_1.S_4)+K_2(S_1.S_3)(S_2.S_4) \end{aligned} \tag{2}$$

where S_i is the spin operator at the ith site of the square plaquette, J_1 is the strength of the n.n. exchange interaction, J_2 that of the diagonal exchange interaction and K_1, K_2 are the strengths of the four-spin exchange interactions.

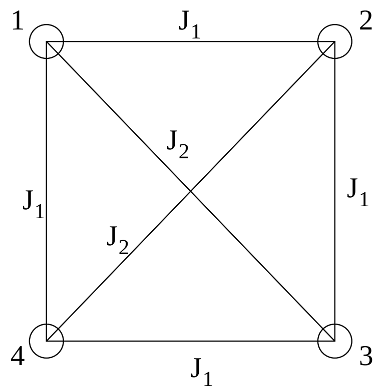

Figure 1: A tetramer of spins of magnitude $\frac{1}{2}$. J_1 and J_2 denote the strengths of the n.n. and diagonal exchange interactions. The four-spin interactions are not shown.

The entanglement properties of the four-spin cluster have earlier been studied analytically only for $J_1 \neq 0$ [37] and numerically for both $J_1 \neq 0, J_2 \neq 0$ [38]. We now determine the entanglement properties analytically for the general case in Eq. (2). The z-component of the total spin, S_z^{tot}, is a conserved quantity so that the eigenvalue problem can be solved in the separate subspaces corresponding to the different values of S_z^{tot}. The results are displayed in the following (E_i , $i = 1, ..., 16$, is the energy eigenvalue):

$S_z^{tot} = +2$

$$\begin{gathered} \psi_1 = |\uparrow\uparrow\uparrow\uparrow\rangle \\ E_1 = \left(J_1 + \frac{J_2}{2} + \frac{K_1}{8} + \frac{K_2}{16}\right) \end{gathered} \tag{3}$$

$S_z^{tot} + 1$

$$\begin{gathered} \psi_2 = \frac{1}{\sqrt{2}}\left(|\uparrow\uparrow\uparrow\downarrow\rangle - |\uparrow\downarrow\uparrow\uparrow\rangle\right) \\ E_2 = -\left(\frac{J_2}{2} + \frac{K_1}{8} + \frac{3K_2}{16}\right) \end{gathered} \tag{4}$$

$$\begin{gathered} \psi_3 = \frac{1}{\sqrt{2}}\left(|\uparrow\uparrow\downarrow\uparrow\rangle - |\downarrow\uparrow\uparrow\uparrow\rangle\right) \\ E_3 = -\left(\frac{J_2}{2} + \frac{K_1}{8} + \frac{3K_2}{16}\right) \end{gathered} \tag{5}$$

$$\begin{gathered} \psi_4 = \frac{1}{\sqrt{4}}\left(|\uparrow\uparrow\uparrow\downarrow\rangle + |\uparrow\uparrow\downarrow\uparrow\rangle + |\uparrow\downarrow\uparrow\uparrow\rangle + |\downarrow\uparrow\uparrow\uparrow\rangle\right) \\ E_4 = \left(J_1 + \frac{J_2}{2} + \frac{K_1}{8} + \frac{K_2}{16}\right) \end{gathered} \tag{6}$$

$$\begin{gathered} \psi_5 = \frac{1}{\sqrt{4}}\left(|\uparrow\uparrow\uparrow\downarrow\rangle + |\uparrow\downarrow\uparrow\uparrow\rangle - |\uparrow\uparrow\downarrow\uparrow\rangle - |\downarrow\uparrow\uparrow\uparrow\rangle\right) \\ E_5 = \left(-J_1 + \frac{J_2}{2} - \frac{3K_1}{8} + \frac{K_2}{16}\right) \end{gathered} \tag{7}$$

$S_z^{tot} = 0$

$$\begin{gathered} \psi_6 = \frac{1}{\sqrt{2}}\left(|\uparrow\uparrow\downarrow\downarrow\rangle - |\downarrow\downarrow\uparrow\uparrow\rangle\right) \\ E_6 = -\left(\frac{J_2}{2} + \frac{K_1}{8} + \frac{3K_2}{16}\right) \end{gathered} \tag{8}$$

$$\begin{aligned} \psi_7 &= \tfrac{1}{\sqrt{2}} \left(|\uparrow\downarrow\downarrow\uparrow\rangle - |\downarrow\uparrow\uparrow\downarrow\rangle \right) \\ E_7 &= -\left(\tfrac{J_2}{2} + \tfrac{K_1}{8} + \tfrac{3K_2}{16} \right) \end{aligned} \tag{9}$$

$$\begin{aligned} \psi_8 &= \tfrac{1}{\sqrt{2}} \left(|\uparrow\downarrow\uparrow\downarrow\rangle - |\downarrow\uparrow\downarrow\uparrow\rangle \right) \\ E_8 &= \left(-J_1 + \tfrac{J_2}{2} - \tfrac{3K_1}{8} + \tfrac{K_2}{16} \right) \end{aligned} \tag{10}$$

$$\begin{aligned} \psi_9 &= \tfrac{1}{\sqrt{6}} \left(|\uparrow\uparrow\downarrow\downarrow\rangle + |\uparrow\downarrow\downarrow\uparrow\rangle + |\downarrow\downarrow\uparrow\uparrow\rangle + |\downarrow\uparrow\uparrow\downarrow\rangle + |\uparrow\downarrow\uparrow\downarrow\rangle + |\downarrow\uparrow\downarrow\uparrow\rangle \right) \\ E_9 &= \left(J_1 + \tfrac{J_2}{2} + \tfrac{K_1}{8} + \tfrac{K_2}{16} \right) \end{aligned} \tag{11}$$

$$\begin{aligned} \psi_{10} &= \tfrac{1}{\sqrt{4}} \left(|\uparrow\uparrow\downarrow\downarrow\rangle + |\downarrow\downarrow\uparrow\uparrow\rangle - |\uparrow\downarrow\downarrow\uparrow\rangle - |\downarrow\uparrow\uparrow\downarrow\rangle \right) \\ E_{10} &= \left(-\tfrac{3J_2}{2} + \tfrac{3K_1}{8} + \tfrac{9K_2}{16} \right) \end{aligned} \tag{12}$$

$$\begin{aligned} \psi_{11} &= \tfrac{1}{\sqrt{12}} \left(2\,|\uparrow\downarrow\uparrow\downarrow\rangle + 2\,|\downarrow\uparrow\downarrow\uparrow\rangle - |\uparrow\uparrow\downarrow\downarrow\rangle - |\uparrow\downarrow\downarrow\uparrow\rangle - |\downarrow\downarrow\uparrow\uparrow\rangle - |\downarrow\uparrow\uparrow\downarrow\rangle \right) \\ E_{11} &= \left(-2J_1 + \tfrac{J_2}{2} + \tfrac{7K_1}{8} + \tfrac{K_2}{16} \right) \end{aligned} \tag{13}$$

$S_z^{tot} = -1$

$$\begin{aligned} \psi_{12} &= \tfrac{1}{\sqrt{2}} \left(|\downarrow\downarrow\downarrow\uparrow\rangle - |\downarrow\uparrow\downarrow\downarrow\rangle \right) \\ E_{12} &= -\left(\tfrac{J_2}{2} + \tfrac{K_1}{8} + \tfrac{3K_2}{16} \right) \end{aligned} \tag{14}$$

$$\begin{aligned} \psi_{13} &= \tfrac{1}{\sqrt{2}} \left(|\downarrow\downarrow\uparrow\downarrow\rangle - |\uparrow\downarrow\downarrow\downarrow\rangle \right) \\ E_{13} &= -(\tfrac{J_2}{2} + \tfrac{K_1}{8} + \tfrac{3K_2}{16}) \end{aligned} \tag{15}$$

$$\begin{aligned} \psi_{14} &= \tfrac{1}{\sqrt{4}} \left(|\downarrow\downarrow\downarrow\uparrow\rangle + |\downarrow\downarrow\uparrow\downarrow\rangle + |\downarrow\uparrow\downarrow\downarrow\rangle + |\uparrow\downarrow\downarrow\downarrow\rangle \right) \\ E_{14} &= \left(J_1 + \tfrac{J_2}{2} + \tfrac{K_1}{8} + \tfrac{K_2}{16} \right) \end{aligned} \tag{16}$$

$$\begin{aligned} \psi_{15} &= \tfrac{1}{\sqrt{4}} \left(|\downarrow\downarrow\downarrow\uparrow\rangle + |\downarrow\uparrow\downarrow\downarrow\rangle - |\downarrow\downarrow\uparrow\downarrow\rangle - |\uparrow\downarrow\downarrow\downarrow\rangle \right) \\ E_{15} &= \left(-J_1 + \tfrac{J_2}{2} - \tfrac{3K_1}{8} + \tfrac{K_2}{16} \right) \end{aligned} \tag{17}$$

$S_z^{tot} = -2$

$$\begin{aligned} \psi_{16} &= |\downarrow\downarrow\downarrow\downarrow\rangle \\ E_{16} &= \left(J_1 + \tfrac{J_2}{2} + \tfrac{K_1}{8} + \tfrac{K_2}{16} \right) \end{aligned} \tag{18}$$

We first discuss the ground state ($T = 0$) entanglement properties. There are five distinct eigenvalues:

$$\begin{aligned} e_1 = E_1 = E_4 = E_9 = E_{14} = E_{16} &= (J_1 + \tfrac{J_2}{2} + \tfrac{K_1}{8} + \tfrac{K_2}{16}) \\ e_2 = E_2 = E_3 = E_6 = E_7 = E_{12} = E_{13} &= -\left(\tfrac{J_2}{2} + \tfrac{K_1}{8} + \tfrac{3K_2}{16} \right) \\ e_3 = E_5 = E_8 = E_{15} &= \left(-J_1 + \tfrac{J_2}{2} - \tfrac{3K_1}{8} + \tfrac{K_2}{16} \right) \\ e_4 = E_{10} &= \left(-\tfrac{3J_2}{2} + \tfrac{3K_1}{8} + \tfrac{9K_2}{16} \right) \\ e_5 = E_{11} &= \left(-2J_1 + \tfrac{J_2}{2} + \tfrac{7K_1}{8} + \tfrac{K_2}{16} \right) \end{aligned} \tag{19}$$

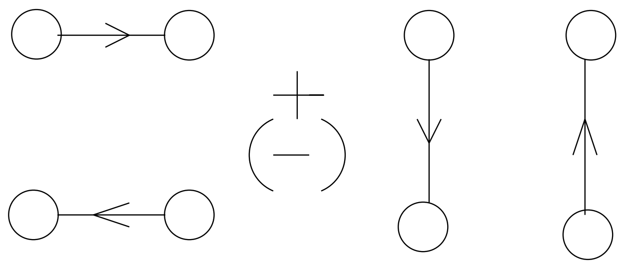

Figure 2: The two resonating valence bond (RVB) states, ψ_{RVB1}(+ sign) and ψ_{RVB2}(- sign). A solid line represents a singlet spin configuration. The arrow convention is explained in the text

For simplicity, let us put $K_1 = K_2 = K$. When $J_2 < J_1$ and $K < \frac{4J_1}{5}$, the ground state is non-degenerate with eigenvalue e_5. When $J_2 < J_1$ and $K > \frac{4J_1}{5}$, the ground state is three-fold degenerate with eigenvalue e_3. Thus $K = \frac{4J_1}{5}$ $(J_2 < J_1)$ is a QCP. When $J_1 < J_2$ and $K < \frac{4J_2}{5}$, the ground state is non-degenerate with eigenvalue e_4. When $J_1 < J_2$ and $K > \frac{4J_2}{5}$, the ground state is six-fold degenerate with eigenvalue e_2 . In this case a QPT occurs at $K = \frac{4J_2}{5}$. With $K < \frac{4J_1}{5}$, a QPT occurs at $J_1 = J_2$ when the ground state changes from ψ_{11} to ψ_{10}. In this paper, we focus our attention on this last QPT. The states ψ_{11} and ψ_{10} describe two resonating valence bond (RVB) states, ψ_{RVB1} and ψ_{RVB2} respectively. Figure 2 gives a pictorial representation of ψ_{RVB1} and ψ_{RVB2}. The solid lines represent singlets (valence bonds) and the arrow signs follow the phase convention that a VB between the sites i and j represents the spin configuration $\frac{1}{\sqrt{2}}\left[\left|\uparrow(i)\downarrow(j)\right\rangle - \left|\downarrow(i)\uparrow(j)\right\rangle\right]$, if the arrow points away from the site i.

A measure of entanglement between the spins at sites i and j is given by concurrence [7, 8]. To calculate this, a knowledge of the reduced density matrix ρ_{ij} is required. This is obtained from the ground state wave function by tracing out all the spin degrees of freedom except those of the spins at the sites i and j. Let ρ_{ij} be defined as a matrix in the standard basis $\{\left|\uparrow\uparrow\right\rangle, \left|\uparrow\downarrow\right\rangle, \left|\downarrow\uparrow\right\rangle, \left|\downarrow\downarrow\right\rangle\}$. One can define the spin-reversed density matrix as $\widetilde{\rho} = (\sigma_y \otimes \sigma_y)\,\rho^*\,(\sigma_y \otimes \sigma_y)$, where σ_y is the Pauli matrix. The concurrence C is given by $C = max\{\lambda_1 - \lambda_2 - \lambda_3 - \lambda_4, 0\}$, where the λ_i's are the square roots of the eigenvalues of the matrix $\rho\widetilde{\rho}$ in descending order. $C = 0$ implies an unentangled state whereas $C = 1$ corresponds to maximum entanglement. The reduced density matrix in the standard basis has the structure

$$\rho_{ij} = \begin{pmatrix} u & 0 & 0 & 0 \\ 0 & \omega_1 & y^* & 0 \\ 0 & y & \omega_2 & 0 \\ 0 & 0 & 0 & v \end{pmatrix} \tag{20}$$

and the concurrence C_{ij} has the simple form

$$C_{ij} = 2\ max\left(0, |y| - \sqrt{uv}\right) \tag{21}$$

If the ground state is degenerate, the $T = 0$ ensemble is described by a density matrix which is an equal mixture of contributions from all possible ground states. The density matrix is a limiting case of the thermal density matrix as $T \to 0$. The state ψ_{RVB1} is the ground state for $J_2 < J_1$ and $K < \frac{4J_1}{5}$. In this case, the n.n. concurrences $C_{12} = C_{23} = C_{34} = C_{41} = 0.5$, i.e., the n.n. spin pairs are entangled in equal amounts. The magnitude of the concurrence is independent of J_1, J_2 and K as long as ψ_{RVB1} remains the ground state. The concurrences C_{13} and C_{24} are zero, i.e., the spins at the ends of a diagonal are unentangled. At the QCP, $J_1 = J_2 = J$ ($K < \frac{4J}{5}$), the concurrences $C_{12}, C_{23}, C_{34}, C_{41}$ and C_{13}, C_{24} are all equal to zero. The ground state at this point is doubly degenerate with wave functions ψ_{RVB1} and ψ_{RVB2}. For $J_2 > J_1$ and $K < \frac{4J_2}{5}$, the ground state is given by ψ_{RVB2}. The n.n. concurrences C_{12}, C_{23}, C_{34} and C_{41} are now zero whereas $C_{13} = C_{24} = 1$. The spin configuration described by ψ_{RVB2} (Fig. 2) can alternatively be described as consisting of VBs, i.e., singlets across the diagonals. Since a singlet is maximally entangled, $C_{13} = C_{24} = 1$. The entanglement properties of a system can further be analyzed in terms of a quantity known as the one-tangle τ_1 which is a measure of the entanglement between a spin and the remainder of the system [39, 40, 41]. It is given as $\tau_1 = 4det\rho^{(1)}$ where $\rho^{(1)}$ is the single-site reduced density matrix. In a translationally invariant system, τ_1 provides a global estimate of the entanglement present whereas the concurrence gives a measure of the pairwise entanglement between two individual spins. When $\tau_1 = 0$, there is no entanglement in the ground state, i.e., the state becomes separable. The Coffman-Kundu-Wootters (CKW) conjecture [39], originally proposed for a three-qubit system, can be generalized to yield the inequality

$$\tau_1 \geq \tau_2 = \sum_{j \neq i} C_{ij}^2 \tag{22}$$

where τ_1 represents the one-tangle corresponding to the entanglement between the ith qubit (spin) and the rest of the system and C_{ij}^2 is the square of the concurrence associated with the pairwise entanglement between the ith and jth qubits. The inequality in (22) shows that the pairwise entanglement is not the sole entanglement in the system. For the four-spin cluster, τ_1 has the value 1 when ψ_{RVB1} and/or ψ_{RVB2} are the ground states. The ratio $R = \frac{\tau_2}{\tau_1}$ quantifies the relative contribution of the pairwise entanglement and has values $\frac{1}{2}$ and 1 in the ground states ψ_{RVB1} and ψ_{RVB2} respectively. Roscilde et al. [40, 41] have shown that the value of R reaches a minimum (not zero) at the QCP of $S = \frac{1}{2}$ XYX AFMs in an external magnetic field. In the present case, we have a first order QPT. At the transition point $J_1 = J_2 = J$ ($K < \frac{4J}{5}$), the ground state is doubly degenerate so that the system is in a mixed state. The entanglement measure τ_1, defined for pure states, needs to be generalized to the case of mixed states. This is done [39] by considering all possible pure state decompositions of the density matrix ρ. For each of the decompositions, one can determine the average value of τ_1. The minimum of the average over all decompositions is taken to be τ_1^{min} which replaces τ_1 in the CKW inequality in Eq. (22). While calculation of τ_1^{min} is difficult, one can readily see that R ($R = \frac{\tau_2}{\tau_1^{min}}$) at the QPT point either has the value zero (τ_2=0, $\tau_1^{min}\neq$0) or is undefined (τ_2=0, τ_1^{min}=0) . In the former case, the value of R reaches a minimum at the transition point. In both the cases R has distinct values on both sides of the transition point. In ψ_{RVB1}, two-spin entanglements exhaust the one-tangle whereas the opposite is true in the case of ψ_{RVB2}. A clearer signature of first order QPT is provided by the jumps in both the n.n. and diagonal concurrences [18, 23]. In the present model, the n.n. concurrences C_{12}, C_{23}, C_{34} and C_{14} are equal to 0.5 in the ground state ψ_{RVB1} and zero at the transition point as well as in the ground state ψ_{RVB2}. The diagonal concurrences C_{13} and C_{24} are equal to 1 in ψ_{RVB2} and zero at the transition point as well as in the state ψ_{RVB1}. The jumps in the magnitudes of the concurrences are associated with the jumps in the density matrix elements, a typical feature of first order QPTs [18].

We now discuss the finite temperature entanglement properties of the spin tetramer. The thermal density matrix, $\rho(T) = \frac{1}{Z}exp(-\beta H)$ ($\beta = \frac{1}{k_BT}$), now replaces the ground state density matrix with Z denoting the partition function of the system. The reduced thermal density matrix $\rho_{ij}(T)$ has the same form as in (20) with $C_{ij}(T)$ given by

$$C_{ij}(T) = \frac{2}{Z}max\left(0, |y(T)| - \sqrt{u(T)v(T)}\right) \tag{23}$$

For the four-spin cluster, the thermal density matrix is

$$\rho(T) = \frac{1}{Z}\sum_{k=1}^{16} exp(-\beta E_k)\left|\psi_k\right\rangle\left\langle\psi_k\right| \tag{24}$$

where the $|\psi_k\rangle's$ and the $E_k's$ are given in equations (3)-(18). The matrix elements u, v and y of the reduced thermal density matrix $\rho_{12}(T)$ are

$$\begin{aligned} u = v = \tfrac{5}{3}e^{-\beta e_1} + \tfrac{3}{2}e^{-\beta e_2} + \tfrac{1}{2}e^{-\beta e_3} + \tfrac{1}{4}e^{-\beta e_4} + \tfrac{1}{12}e^{-\beta e_5} \\ y = \tfrac{5}{6}e^{-\beta e_1} - \tfrac{1}{2}e^{-\beta e_3} - \tfrac{1}{3}e^{-\beta e_5} \end{aligned} \tag{25}$$

where the eigenvalues $e_i's$ ($i = 1, 2, ..., 5$) are given in Eq. (19). Due to translational invariance, the reduced density matrices for the other n.n. spin pairs have the same matrix elements as in the case of $\rho_{12}(T)$. Figure 3 shows C_{12} as a function of $\frac{k_BT}{J_1}$ for $\frac{J_2}{J_1} = 0.5$ and for $r = \frac{K}{J_1}$ ($K_1 = K_2 = K$) $= 0.4$ (a), 0.2 (b) and 0.0 (c). Increase in the strength of the four-spin interaction reduces the magnitude of the n.n. concurrence. The value of the concurrence is non-zero provided $|y| - \sqrt{uv}$ (Eq.(23)) is > 0. One can define a critical temperature T_c beyond which the entanglement between n.n. spins disappears [37, 42]. One can show

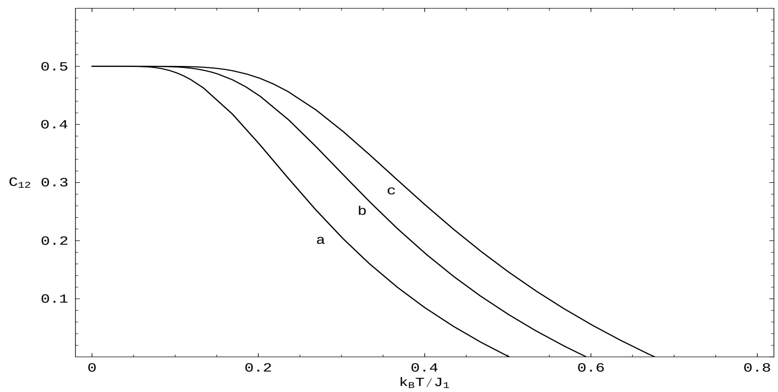

Figure 3: Concurrence C_{12} as a function of $\frac{k_B T}{J_1}$ for $\frac{J_2}{J_1} = 0.5$ and for $r = \frac{K}{J_1}(K_1 = K_2 = K) = 0.4$ (a), 0.2 (b) and 0.0 (c).

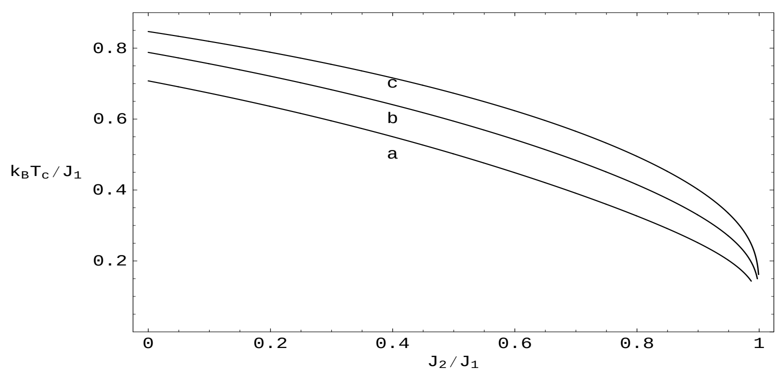

Figure 4: A plot of $\frac{k_B T_c}{J_1}$, where T_c is the critical entanglement temperature, versus $\frac{J_2}{J_1}$, for $r = 0.4$ (a), 0.2 (b) and 0.0 (c)

that in the parameter regime of interest, the thermal entanglement between the diagonal spins is zero so that T_c can be taken as the critical temperature beyond which the entanglement between any two spins is zero. The critical temperature T_c is obtained from $|y| - \sqrt{uv} = 0$ (Eq. (23)), i.e., as a solution of the equation

$$z^{3-\frac{3r_2}{4}} - 6z^{1+r_1+\frac{r_2}{2}} - z^{1+2r_1-\frac{3r_2}{4}} - 10 = 0 \tag{26}$$

where $z = e^{\frac{J_1}{k_B T}}, r_1 = \frac{J_2}{J_1}$ and $r_2 = \frac{K}{J_1}$. Figure 4 shows a plot of $\frac{k_B T_c}{J_1}$ versus $\frac{J_2}{J_1}$ for $r = 0.4$ (a), 0.2 (b) and 0.0 (c). For a fixed value of $\frac{J_2}{J_1}$, the critical entanglement temperature T_c decreases as the strength of the four-spin interaction increases. T_c tends to zero as $\frac{J_2}{J_1}$ approaches the QCP $\frac{J_2}{J_1} = 1$. For $J_2 > J_1$ (with $K < \frac{4J_2}{5}$), the n.n. concurrences are zero.

We next calculate the concurrence for pairwise entanglement between the spins located at the ends of a diagonal. The matrix elements u, v and y of the reduced thermal density matrix $\rho_{13}(T)$ are given by

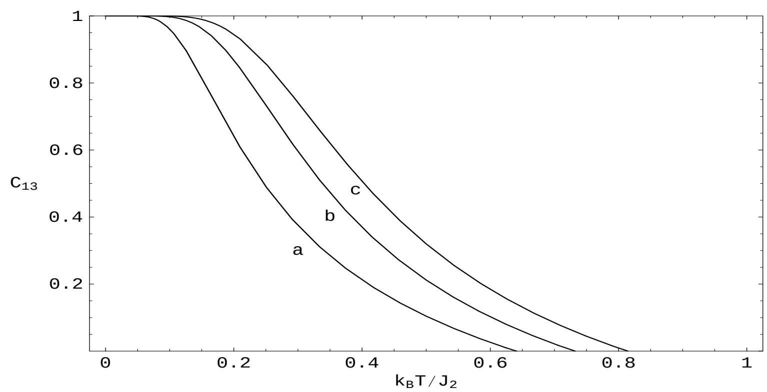

Figure 5: Concurrence C_{13} as a function of $\frac{k_BT}{J_2}$ for $\frac{J_2}{J_1} = 0.5$ and for $r = \frac{K}{J_1}(K_1 = K_2 = K) = 0.4$ (a), 0.2 (b) and 0.0 (c).

$$
\begin{aligned}
u = v &= \tfrac{5}{3}e^{-\beta e_1} + e^{-\beta e_2} + e^{-\beta e_3} + \tfrac{1}{3}e^{-\beta e_5} \\
y &= \tfrac{5}{6}e^{-\beta e_1} - e^{-\beta e_2} + \tfrac{1}{2}e^{-\beta e_3} - \tfrac{1}{2}e^{-\beta e_4} + \tfrac{1}{6}e^{-\beta e_5}
\end{aligned}
\tag{27}
$$

where the eigenvalues $e_i{}'s$ are given in Eq. (19). The reduced density matrix $\rho_{24}(T)$ has the same elements as in the case of $\rho_{13}(T)$. Figure 5 shows C_{13} as a function of $\frac{k_BT}{J_2}$ for $\frac{J_1}{J_2} = 0.5$ and for $r = \frac{K}{J_2}(K_1 = K_2 = K) = 0.4$ (a), 0.2 (b) and 0.0 (c). Again, at a fixed value of $\frac{J_1}{J_2}$, the magnitude of C_{13} decreases as the strength of the four-spin interaction increases. The critical entanglement temperature T_c, beyond which the entanglement between spins located at the ends of a diagonal disappears, is also the temperature beyond which the pairwise entanglement between any two spins vanishes since in the parameter regime of interest the n.n. concurrences are zero at all T. The critical temperature T_c is obtained as a solution of the equation

$$
z^{2+r_1-\frac{3r_2}{4}} - 3z^{2r_1+\frac{r_2}{2}} - z^{3r_1-\frac{3r_2}{4}} - 5 = 0 \tag{28}
$$

where $z = e^{\frac{J_2}{k_BT}}, r_1 = \frac{J_1}{J_2}$ and $r_2 = \frac{K}{J_2}$. Figure 6 shows a plot of $\frac{k_BT_c}{J_2}$ versus $\frac{J_1}{J_2}$ for $r = 0.4$ (a), 0.2 (b) and 0.0 (c). For a fixed value of $\frac{J_1}{J_2}$, the critical entanglement temperature T_c decreases as the strength of the four-spin interaction K increases. T_c approaches zero as $\frac{J_1}{J_2}$ approaches the QCP $\frac{J_1}{J_2} = 1$. The major conclusion one arrives at from an examination of Figs. (3)-(6), is that, as in the $T = 0$ case, the two sets of concurrences (i) $C_{12}, C_{23}, C_{34}, C_{41}$ and (ii) $C_{13,}, C_{24}$ are mutually exclusive. For finite values of the concurrences belonging to the first set, the values of the concurrences belonging to the second set are zero and vice versa.

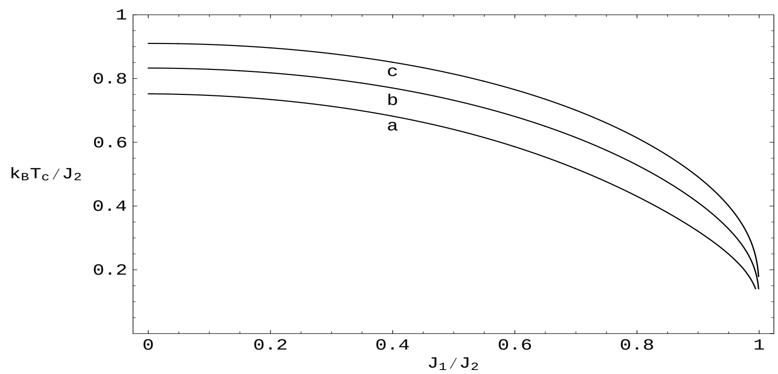

Figure 6: A plot of $\frac{k_B T_c}{J_2}$, where T_c is the critical entanglement temperature, versus $\frac{J_1}{J_2}$, for $r = 0.4$ (a), 0.2 (b) and 0.0 (c).

III. Entanglement Witness

We now consider the $S = \frac{1}{2}$ polyoxovanadate AFM compound $V12$ and show that the magnetic susceptibility χ serves as an EW for this compound. The magnetic properties of this system are well described by considering only the central square of localized V^{4+}ions [36]. These ions form a square plaquette of $S = \frac{1}{2}$ localized spins described by the isotropic Heisenberg AFM Hamiltonian with only n.n. interactions ($J_2 = K_1 = K_2 = 0$ in equation (2)). As shown in Ref. [36], the $V12$ compound can be treated as a collection of independent $S = \frac{1}{2}$ tetramers with AFM n.n. interactions of strength $\frac{J_1}{k_B} \simeq 17.6$ K. In fact, the theoretical expression for the magnetic susceptibility χ of a tetramer gives a good fit (N independent tetramers are to be considered in calculating χ) to the experimental data for $V12$ (Fig. 2 of Ref. [36]). The susceptibility for a spin tetramer with only n.n. interaction of strength J_1 is given by

$$\frac{\chi}{(g\mu_B)^2/J_1} = \beta J_1 \frac{10e^{-3\beta J_1} + 4e^{-2\beta J_1} + 2e^{-\beta J_1}}{1 + e^{-2\beta J_1} + 3e^{-\beta J_1} + 6e^{-2\beta J_1} + 5e^{-3\beta J_1}} \tag{29}$$

Following Ref. [28], the magnetic susceptibility, χ_α, along the direction α ($\alpha = x, y, z$) can be written as

$$\chi_\alpha = \frac{(g\mu_B)^2}{k_B T} \left\langle (M_\alpha)^2 \right\rangle \tag{30}$$

where $M_\alpha = \sum_j S_j^\alpha$ denotes the magnetization along α. The expression in (30) holds true when the external magnetic field is zero and the Hamiltonian is isotropic in spin space. The angular brackets in (30) denote the thermal expectation value. The susceptibility χ_α can further be written as

$$\chi_\alpha = \frac{(g\mu_B)^2}{k_B T} \sum_{i,j} \left\langle S_i^\alpha S_j^\alpha \right\rangle \tag{31}$$

Due to the isotropy of the Hamiltonian, $\chi_x = \chi_y = \chi_z = \chi$ and we can write

$$\chi = \frac{(g\mu_B)^2}{k_B T} [\frac{N}{4} + \frac{2}{3} \sum_{i<j} \langle S_i.S_j \rangle] \tag{32}$$

where N is the total number of interacting spins. The summation of expectation values in (32) can be considered as the expectation value of the sum H_S of interaction terms describing all-to-all spin couplings. The expectation value of H_S has an overall negative contribution to χ because of AFM correlations. H_S has the nature of a Hamiltonian and the maximum negative expectation value is given by the ground state energy of H_S. For separable states, the energy minimum is given by the ground state energy of the equivalent classical Hamiltonian [32, 33]. For all-to-all spin couplings, the minimum energy separable state is described by any spin configuration with total spin vector zero. For N=4 (spin tetramer), the classical ground state is given by the Néel state and $\langle H_S \rangle = -\frac{1}{2}$. For general separable states, $\langle H_S \rangle$ has a lesser negative contribution to χ and one can write down the inequality

$$\chi \geq \frac{(g\mu_B)^2}{k_B T} \frac{2}{3} \tag{33}$$

for separable, i.e., unentangled states. Figure 7 shows a plot of $\frac{\chi}{n(g\mu_B)^2/J_1}$ versus T (Curve a) for n independent tetramers, the case of $V12$. The expression for the susceptibility of a single tetramer is given in (29). Curve b represents the χ versus T curve describing the equality in (33). In plotting the curves, the value of $\frac{J_1}{k_B}$ is taken as 17.6 K, the experimental estimate for $V12$. The intersection point of the two curves provides an estimate, $T_c \simeq 25.4$ K, of the critical entanglement temperature below which entanglement is present in $V12$. The theoretical value of the critical temperature, above which the two-spin entanglement disappears is obtained from Eq. (26), with $r_1 = r_2 = 0$, as $T_c^{(1)} \simeq 15.2$ K. Since $T_c > T_c^{(1)}$, only multipartite entanglement is present in the thermal state of the tetramer for $T_c^{(1)} < T < T_c$.

We now examine whether four-spin entanglement exists in the thermal state of the tetramer. This is done by calculating the state preparation fidelity F defined as

$$F(\rho) = \langle \psi_{GHZ} | \, \rho(T) \, | \psi_{GHZ} \rangle \tag{34}$$

where $|\psi_{GHZ}\rangle = \frac{1}{\sqrt{2}} (|\uparrow\downarrow\uparrow\downarrow\rangle + |\downarrow\uparrow\downarrow\uparrow\rangle)$ is the four-spin Greenberger-Horne-Zeilinger (GHZ) state [37]. The sufficient condition for the four-particle ($N = 4$) entan-

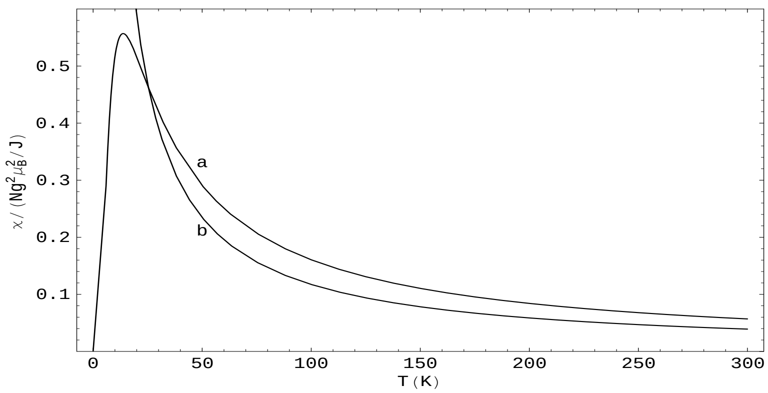

Figure 7: A plot of $\frac{\chi}{n(g\mu_B)^2/J_1}$ (dimensionless unit) versus T (Curve a) for n independent tetramers, as is the case of $V12$. Curve b represents the χ versus T curve describing the equality in (33). The intersection point of the two curves represents the critical entanglement temperature $T_c \simeq 25.4$ K with $\frac{J_1}{k_B} \simeq 17.6$ K.

glement is given by

$$F(\rho) > \frac{1}{2} \tag{35}$$

For a tetramer with only n.n. interactions of strength J_1, $F(\rho)$ is calculated as

$$F(\rho) = \frac{\frac{1}{3}e^{-\beta J_1} + \frac{2}{3}e^{2\beta J_1}}{5e^{-\beta J_1} + 7 + 3e^{\beta J_1} + e^{2\beta J_1}} \tag{36}$$

$F(\rho) = \frac{2}{3}$,i.e., $> \frac{1}{2}$ as $T \to 0$ indicating the presence of four-spin entanglement in the ground state of the tetramer. The critical entanglement temperature, $T_c^{(4)}$, beyond which the four-spin entanglement vanishes is obtained from a solution of the equation $F(\rho) = \frac{1}{2}$. The value obtained is $\frac{k_B T_c^{(4)}}{J_1} \simeq 0.417$ from which $T_c^{(4)} \simeq 7.4$ K, assuming $\frac{J_1}{k_B} \simeq 17.6$ K as in the case of the compound $V12$. One finds that $T_c^{(4)}$ is less than the critical temperature $T_c^{(1)} \simeq 15.2$ K. We next consider a tetramer with n.n., diagonal and four-spin exchange interactions of strength J_1, J_2 and $K_1 = K_2 = K$ respectively. Fig. 8 shows a plot of $\frac{k_B T_c^{(4)}}{J_1}$ versus $\frac{J_2}{J_1}$ for $r = \frac{K}{J_1} = 0.4$ (a), 0.2 (b) and 0.0 (c) respectively. For a fixed value of $\frac{J_2}{J_1}$, the critical temperature for four-spin entanglement decreases as the strength of the four-spin interaction increases.

The tetramer with $J_1 = J_2 = J$ and $K = 0$, alternatively described as the tetrahedron, provides an interesting example of the magnetic susceptibility χ serving as a witness for entanglement other than the entanglement between individual spins. The two-spin entanglement vanishes in the thermal state of the tetrahedron. The same is true when $T = 0$ and the system is at the QCP $J_1 = J_2$. Figure 9 shows the EW curves for χ (the same inequality bound as in (33) holds true) which intersect at a finite temperature $\frac{k_B T_c}{J} \simeq 1.9$ showing that the thermal

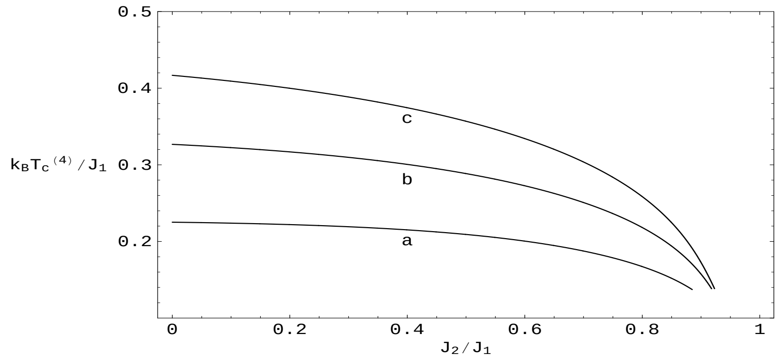

Figure 8: Plot of $\frac{k_B T_c^{(4)}}{J_1}$ versus $\frac{J_2}{J_1}$ for $r = \frac{K}{J_1} = 0.4$ (a), 0.2 (b) and 0.0 (c). $T_c^{(4)}$is the critical entanglement temperature above which the four-spin entanglement is zero.

states are entangled below the critical temperature corresponding to the intersection point. The entanglement is exclusively multipartite in nature. Figure 10 shows the EW curves for χ in the case of a symmetric trimer described by the $S = \frac{1}{2}$ Heisenberg AFM Hamiltonian

$$H_{trimer} = J(S_1.S_2 + S_2.S_3 + S_3.S_1) \tag{37}$$

In this case, it is well-known [37, 43] that there is no pairwise entanglement both at $T = 0$ and at finite temperatures. In the inequality for χ (Eq.(33)), the factor $\frac{2}{3}$ is replaced by the factor $\frac{1}{2}$. In the classical ground state of H_S, the interacting spins form angles of $\frac{2\pi}{3}$ with each other. The critical temperature is given by $\frac{k_B T_c}{J} \simeq 1.4$. Again, only multipartite entanglement is present in the thermal state of the symmetric trimer.

Another EW, which provides an estimate of critical entanglement temperature T_c, is based on energy [32, 33]. The entanglement gap G_E is defined as

$$G_E = E_{sep} - E_0 \tag{38}$$

where E_0 is the ground state energy of the Hamiltonian H describing the system and E_{sep} is the minimum energy of the separable states. If G_E is > 0, a finite energy range exists over which all states are entangled. For a positive entanglement gap $G_E > 0$, one can define an EW

$$Z_{EW} = H - E_{sep} I \tag{39}$$

where I represents the identity on the full Hilbert space. For any separable state, $Tr(Z_{EW}\rho_{sep)}) \geq 0$. If the state is entangled, $Tr(Z_{EW}\rho_{ent)})$ is < 0. For example, if the state belongs to the ground state manifold, $Tr(Z_{EW}\rho_0) = E_0 - E_{sep} < 0$. Z_{EW} thus acts as an EW.The entanglement gap temperature T_E is given by $U(T_E) =$

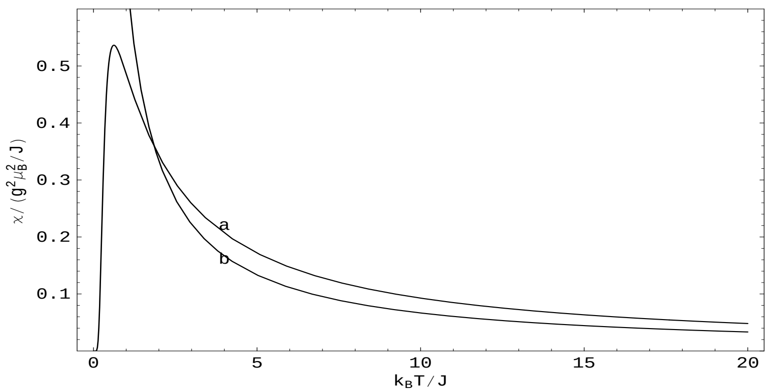

Figure 9: The EW curves for χ in the case of a symmetric tetrahedron with $J_1 = J_2 = J$ and $K = 0$.

E_{sep}, where $U(T)$ $(= \langle H \rangle = -\frac{1}{Z}\frac{\partial Z}{\partial \beta})$ is the thermal energy at temperature T. For $T < T_E$, the thermal state is entangled and hence T_E is a measure of the critical entanglement temperature. E_{sep} is given by the ground state energy of the corresponding classical spin model [32, 33]. For a square of spins, $E_{sep} = -J_1$, as the classical ground state is given by the Néel state. The expression for $U(T)$ is obtained from the partition function Z of the square of spins As shown in [33], in the case of bipartite graphs and lattices, the EW detects only bipartite entanglement. Thus T_E for the square of spins has an identical magnitude as that of $T_c^{(1)}$ at and above which such entanglement vanishes. In the case of non-bipartite graphs and lattices, the EW can detect multipartite entanglement. The tetrahedron and the symmetric trimer are examples of non-bipartite graphs. E_{sep} in these two cases can readily be calculated as $E_{sep} = -0.5J$ (tetrahedron) and $E_{sep} = -\frac{3}{8}J$ (symmetric trimer). The entanglement temperature T_E has the magnitude $\frac{k_B T_E}{J} \simeq 1.9$ (tetrahedron) and $\frac{k_B T_E}{J} \simeq 1.4$ (symmetric trimer). In both the cases, two-spin entanglements are absent and the entanglement present in the system for $T < T_E$ is multipartite in nature.

IV. Summary and Discussion

In this paper, we consider a spin tetramer ($S = \frac{1}{2}$) with n.n., diagonal and four-spin AFM exchange interactions of strength J_1, J_2 and $K_1 = K_2 = K$ respectively. The significance of the inclusion of three-spin and four-spin interactions in spin Hamiltonians of interest has been pointed out earlier [44, 45]. We study the ground state and thermal entanglement properties of the tetramer in the various limiting cases. At $T = 0$, QPTs occur as the exchange interaction strengths are tuned to certain critical values.We focus on a particular QPT at $J_1 = J_2 = J$ ($K < \frac{4}{5}J$) as the other QPTs exhibit similar features. The QPT point separates two RVB ground states, ψ_{RVB1} and ψ_{RVB2}. The entanglement between two spins

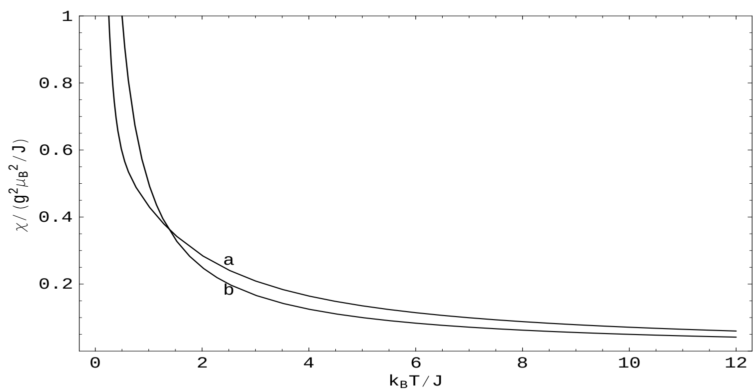

Figure 10: The EW curves for χ in the case of the symmetric trimer.

is determined by calculating the concurrences $C_{12}, C_{23}, C_{34}, C_{41}$ and C_{13}, C_{24}. The n.n. concurrences are non-zero only in ψ_{RVB1} and the other two concurrences associated with diagonal spins are non-zero only in ψ_{RVB2}. The $1-$tangle τ_1, a measure of the global entanglement, has the value 1 in both ψ_{RVB1} and ψ_{RVB2}. The entanglement measure τ_1, defined for pure states, has to be generalized to τ_1^{min} at the QPT point where the ground state is doubly degenerate. The entanglement ratio $R = \frac{\tau_2}{\tau_1^{min}}$ has the value zero at the transition point if $\tau_1^{min} \neq 0$ and is undefined otherwise. Away from the transition point, $R = 0.5$ in the ground state ψ_{RVB1} and 1.0 in the ground state ψ_{RVB2}. A better evidence of the first order QPT is provided by the jumps in both the n.n. and diagonal concurrences [18, 23].

The study of finite temperature entanglement properties again shows the existence of two distinctive parameter regimes. The n.n. concurrences are non-zero only when $J_2 < J_1 (K < \frac{4J_1}{5})$ and the concurrences associated with diagonal spins are non-zero only when $J_1 < J_2 (K < \frac{4J_2}{5})$. At $J_1 = J_2$, all the six concurrences are zero. The critical entanglement temperature, T_c, beyond which entanglement between two spins disappears, is computed. The magnitude of T_c is highest when $J_2 = 0$ and $K = 0$. For fixed values of J_1 and J_2, T_c decreases as the strength of the four-spin interaction increases. A measure of the four-spin entanglement in the thermal state of the tetramer is obtained by calculating the fidelity $F(\rho)$. The critical temperature, $T_c^{(4)}$, beyond which the four-spin entanglement disappears is calculated and one finds that at fixed values of J_1 and J_2, the magnitude of $T_c^{(4)}$ decreases as the strength K of the four-spin interaction increases.

Molecular or nanomagnets provide examples of spin systems in which the dominant exchange interactions are confined to small spin clusters like dimers, trimers and tetramers. In several cases, the magnetic properties can be well explained by treating the solid to consist of independent spin clusters. We consider one such compound, $V12$, which is a collection of spin tetramers with only n.n. exchange interactions. Treating the magnetic susceptibility χ as an EW, the critical temperature, T_c, below which entanglement is present in the system, is estimated from the experimental data on χ. The entanglement includes both bipartite and multipartite entanglement with $T_c \simeq 25.4$ K in the case of $V12$ ($\frac{J}{k_B} \simeq 17.6$ K). From theoretical calculations, the critical temperature $T_c^{(1)}$, beyond which bipartite entanglement vanishes is given by $T_c^{(1)} \simeq 15.2$ K. Since $T_c^{(1)} < T_c$, multipartite entanglement in the system persists upto a higher temperature. The entanglement contents of the thermal states of the tetrahedron and the symmetric trimer are shown to be exclusively multipartite in nature. An EW based on energy provides evidence of bipartite entanglement in the case of a square of spins (relevant for $V12$) and multipartite entanglement in the cases of the tetrahedron and the symmetric trimer. The EW based on susceptibility χ can detect both bipartite and multipartite entanglement. The EW based on energy detects only bipartite entanglement when the spin system is defined on a bipartite graph or lattice. The latter EW can detect multipartite entanglement only in the case of a non-bipartite graph or lattice. The critical entanglement temperature T_c and the entanglement gap temperature T_E have identical values if the corresponding EWs both detect entanglement.

After our work was completed, we learnt of a new inequality for susceptibility serving as an EW [47, 48]. The inequality can be derived using the sum uncertainty relation for spin$-\frac{1}{2}$ operators [47, 49]. When $\chi_x = \chi_y = \chi_z = \chi$, the separability criterion for a single cluster of N spins is given by

$$\chi \geq \frac{(g\mu_B)^2}{k_B T}\frac{N}{6} \tag{40}$$

The results reported by us, using slightly different arguments, are special cases of the general condition (40) for $N = 3$ and 4. We can generalize our derivation in the following manner to obtain (40). We start with the identity

$$H_S = \sum_{i<j} S_i S_j = \frac{1}{2}(S^2 - \sum_{i=1}^{N} S_i^2) \tag{41}$$

where $\boldsymbol{S}$ is the total spin vector. The maximum negative contribution to χ is obtained for $\boldsymbol{S}$ =0. Thus for separable states with $\langle S_i^2 \rangle = \frac{1}{4}$, Eq.(32) reduces to the inequality in (40). There is now a wealth of experimental data on molecular magnets and other magnetic systems which are yet to be analyzed in terms of the entanglement properties of the systems [35, 46]. Appropriate finite temperature measures of the different types of entanglement need to be developed so that contact between theory and experiments can be made. A challenging task ahead is to develop suitable EWs which provide signatures of the different types of entanglement in the experimental data.

Acknowledgment. Amit Tribedi is supported by the Council of Scientific and Industrial Research, India under Grant No. 9/15 (306)/ 2004-EMR-I.

References

[1] M. A. Nielsen and I. L. Chuang, Quantum Computation and Quantum Information (Cambridge University Press, Cambridge, 2000)

[2] D. Loss and D. P. DiVincenzo, Phys. Rev. A 57, 120 (1998); G. Burkard, D. Loss and D. P. DiVincenzo, Phys. Rev. B 59, 2070 (1999)

[3] B. E. Kane, Nature 393, 133 (1998)

[4] D. P. DiVincenzo, D. Bacon, J. Kempe, G. Burkard and K. B. Whaley, Nature (London) 408, 339 (2000)

[5] J. J. Garcia-Ripoll, M. A. Martin-Delgado and J. I. Cirac, Phys. Rev. Lett. 93, 250405 (2004)

[6] M. Popp, F. Verstraete, M. A. Martin-Delgado and J. I. Cirac, quant-ph/0411123

[7] K. M. O'Connor and W. K. Wootters, Phys. Rev. A 63, 052302 (2001); W. K. Wootters, Phys. Rev. Lett. 80, 2245 (1998)

[8] M.C . Arnsen, S. Bose ad V. Vedral, Phys. Rev. Lett. 87, 017901 (2001); D. Gunlycke et al., Phys. Rev. A 64, 042302 (2001)

[9] M. A. Nielsen, Ph. D. Thesis, University of Mexico, 1998, quant-ph/0011036

[10] X. Wang, Phys. Rev. A 64, 012313 (2001); Phys. Lett. A 281, 101 (2001)

[11] X. Wang, Phys. Rev. A 66, 034302 (2002)

[12] D. Bruβ, N. Dutta, A. Ekert, L. C. Kwek and C. Macchiavello, quant-ph/0411080

[13] U. Glasser, H. Büttner and H. Fehske, Phys. Rev. A 68, 032318 (2003)

[14] T.-C. Wei, D. Das, S. Mukhopadhyay, S. Vishveshwara and P. M. Goldbart, quant-ph/0405162

[15] A. Osterloh, L. Amico, G. Falci and R. Fazio, Nature (London) 416, 608 (2002)

[16] T. J. Osborne ad M. A. Nielsen, Phys. Rev. A 66, 032110 (2002)

[17] S. Sachdev, Quantum Phase Transitions (Cambridge University Press, Cambridge, 1999)

[18] L.-A. Wu, M. S. Sarandy and D. A. Lidar, Phys. Rev. Lett. 93, 250404 (2004)

[19] J. Vidal, G. Palacios and R. Mosseri, Phys. Rev. A 69, 022107 (2004)

[20] G. Vidal, J. I. Latorre, E. Rico and A. Kitaev, Phys. Rev. Lett. 90, 227902 (2003)

[21] F. Verstraete, M. Popp and J. I. Cirac, Phys. Rev. Lett. 92, 027901 (2004)

[22] R. Somma, G. Ortiz, H. Barnum, E. Knill and L. Viola, Phys. Rev. A 70, 042311 (2004)

[23] I. Bose and E. Chattopadhyay, Phys. Rev. A 66, 062320 (2002)

[24] F. C. Alcaraz, A. Saguia and M. S. Sarandy, Phys. Rev. A70, 032333 (2004)

[25] J. Vidal, R. Mosseri and J. Dukelsky, Phys. Rev. A 69, 054101 (2004)

[26] X.-F.Qian, T. Shi, Y. Li, Z. Song and C.-P. Sun, quant-ph/0502121

[27] S. Ghosh, T. F. Rosenbaum, G. Aeppli and S. N. Coppersmith, Nature 425, 48 (2003); V. Vedral, Nature 425, 28 (2003)

[28] Č. Brukner, V. Vedral and A. Zeilinger, quant-ph/0410138

[29] X. Wang and P. Zanardi, Phys. Lett. A 301, 1 (2002)

[30] V. Vedral, New J. Phys. 6, 22 (2004)

[31] Č. Brukner and V. Vedral, quant-ph/0406040

[32] G. Tóth, quant-ph/0406061

[33] M. R. Dowling, A. C. Doherty and S. D. Bartlett, quant-ph/0408086

[34] L.-A. Wu, S. Bandyopadhyay, M. S. Sarandy and W. A. Lidar, quant-ph/0412099

[35] J. T. Haraldsen, T. Barnes and J. L. Musfeldt, Phys. Rev. B 71, 064403 (2005)

[36] D. Procissi, A. Shastri, I. Rousochatzakis, M. AI Rifafi, P. Kögerler and M. Luban, Phys. Rev. B 69, 094436 (2004)

[37] X. Wang, Phys. Rev. A 66, 044305 (2002)

[38] S.- J. Gu, H. Li, Y.- Q. Li and H. -Q. Lin, quant-ph/0403026

[39] V. Coffman, J. Kundu and W. K. Wootters, Phys. Rev. A 61, 052306 (2000)

[40] T. Roscilde, P. Verrucchi, A. Fubini, S. Haas and V. Tognetti, Phys. Rev. Lett. 93, 167203 (2004)

[41] T. Roscilde, P. Verrucchi, A. Fubini, S. Haas and V. Tognetti, quant-ph/0412098

[42] H. Fu, A. I. Solomon and X. Wang, quant-ph/0401015

[43] X. Wang , H. Fu and A. I. Solomon, J. Phys. A 34, 11307 (2001)

[44] J. K. Pachos and M. B. Plenio, quant-ph/0401106

[45] A. Mizel and D. A. Lidar, quant-ph/0401081

[46] M. U.- Kartin, S.-J. Hwu and J. A. Clayhold, Inorganic Chemistry 42, 2405 (2003)

[47] M. Wieśniak, V. Vedral and Č. Brukner, quant-ph/0503037

[48] T. Vértesi and E. Bene, cond-mat/0503726

[49] H. F. Hofmann and S. Takeuchi, Phys. Rev. A 68, 032103 (2003)